

- (32) F. R. Kreissl, P. Friedrich, and G. Huttner, *Angew. Chem., Int. Ed. Engl.*, **16**, 102 (1977).
- (33) (a) E. W. Abel and R. J. Rowley, *J. Chem. Soc., Dalton Trans.*, 1096 (1975); (b) E. W. Abel, R. J. Rowley, R. Mason, and K. M. Thomas, *J. Chem. Soc., Chem. Commun.*, 72 (1974).
- (34) C. W. Fong and G. Wilkinson, *J. Chem. Soc., Dalton Trans.*, 1100 (1975).
- (35) M. Matsumoto, K. Nakutsu, K. Tani, A. Nakamura, and S. Otsuka, *J. Am. Chem. Soc.*, **96**, 6777 (1974).
- (36) S. S. Crawford, G. Firestein, and H. D. Kaesz, *J. Organomet. Chem.*, **91**, C57 (1975).
- (37) D. T. Sepelak, C. G. Pierpont, E. K. Barefield, J. T. Budz, and C. A. Poffenberger, *J. Am. Chem. Soc.*, **98**, 6178 (1976).
- (38) J. L. Thomas, *J. Am. Chem. Soc.*, **97**, 5943 (1975).
- (39) F. R. Kreissl, C. G. Kreiter, and E. O. Fischer, *Angew. Chem., Int. Ed. Engl.*, **11**, 643 (1972).
- (40) F. R. Kreissl, E. O. Fischer, C. G. Kreiter, and K. Weiss, *Angew. Chem., Int. Ed. Engl.*, **12**, 563 (1973).
- (41) (a) R. Huisgen, B. Giese, and H. Huber, *Tetrahedron Lett.*, 1883 (1967); (b) R. Huisgen, K. Herblg, A. Seigl, and H. Huber, *Chem. Ber.*, **99**, 2526 (1966).
- (42) It is noteworthy that the proposed intermediate enamine ligands in VI and VII isomerize to one-carbon three electron and two-carbon three-electron moieties, respectively in IV and V. As a referee has pointed out, the driving force for the formation of a one-carbon ligand from VI may well be associated with the presence of two bulky groups ($-\text{Ph}$ and $-\text{NHC}_6\text{H}_{11}\text{-c}$) on the β -carbon atom of the intermediate enamine. Formation of a two-carbon ligand from VI may be sterically unfavorable.
- (43) G. N. Mott and A. J. Carty, unpublished results.
- (44) C. J. Lancelot, D. J. Cram, and P. v. R. Schleyer in "Carbonium Ions", Vol. III, G. A. Olah and P. v. R. Schleyer, Ed., Wiley-Interscience, New York, N.Y., 1976, p 1347.

Synthesis and Characterization of Trimethyl Phosphite Derivatives $\text{HFeCo}_3(\text{CO})_{12-x}[\text{P}(\text{OCH}_3)_3]_x$, $x = 1, 2, 3, 4$. Crystal and Molecular Structure of $\text{HFeCo}_3(\text{CO})_9[\text{P}(\text{OCH}_3)_3]_3$ at -139°C ¹

B. T. Huie, C. B. Knobler, and H. D. Kaesz*

Contribution No. 3858 from the Department of Chemistry, University of California, Los Angeles, California 90024. Received July 13, 1977

Abstract: The series of derivatives $\text{HFeCo}_3(\text{CO})_{12-x}[\text{P}(\text{OCH}_3)_3]_x$, $x = 1, 2, 3, 4$, has been synthesized from $\text{HFeCo}_3(\text{CO})_{12}$ and $\text{P}(\text{OCH}_3)_3$ under a variety of conditions. Infrared and Mössbauer spectral data were obtained; ¹H NMR gives satisfactory signals for hydrogen of methyl groups on the ligand but no signals were observed for hydrogen on the metal cluster. The structure of $\text{HFeCo}_3(\text{CO})_9[\text{P}(\text{OCH}_3)_3]_3$ has been determined from data collected at -139°C on an automated diffractometer with monochromatized Mo $K\alpha$ radiation. The compound crystallizes in the monoclinic space group $P2_1/c$ with $a = 16.336(3) \text{ \AA}$, $b = 10.896(2) \text{ \AA}$, $c = 18.583(2) \text{ \AA}$, $\beta = 97.26(1)^\circ$, and $V = 3281(1) \text{ \AA}^3$ at 25°C . The density at 25°C of 1.737 g cm^{-3} calculated on the basis of four molecules per unit cell agrees with the flotation value of 1.72 g cm^{-3} . At -139°C the cell parameters are $a = 15.992(6) \text{ \AA}$, $b = 10.638(3) \text{ \AA}$, $c = 18.403(4) \text{ \AA}$, $\beta = 98.575(25)^\circ$, $V = 3093(3) \text{ \AA}^3$, and $d_{\text{calcd}} = 1.843 \text{ g cm}^{-3}$. The structure was solved by use of direct methods and Fourier summations and the full-matrix, least-squares refinement, based on 6057 independent observed reflections measured at -139°C , converged to a conventional R index of 0.061. The four metal atoms are at the corners of a tetrahedron. Six of the nine carbonyl groups are terminally bound, three to Fe with an average Fe-C distance of 1.798 \AA and one to each Co with an average Co-C distance of 1.755 \AA . The other three carbonyl groups form symmetric Co-C-Co bridges with an average Co-C distance of 1.954 \AA . The molecule has Fe-Co distances averaging 2.560 \AA and Co-Co distances averaging 2.488 \AA . All three trimethyl phosphite ligands are trans to Fe; the average Fe-Co-P angle is 174° . The hydrogen atom is located outside the cluster on the threefold axis in a face-bridging position 0.75 \AA from the Co_3 plane; the average Co-H distance is $1.63(15) \text{ \AA}$. The molecular threefold axis lies approximately parallel to the c axis in the crystal.

Introduction

The tetranuclear mixed metal carbonyl hydride $\text{HFeCo}_3(\text{CO})_{12}$ was first synthesized and characterized by Chini et al. in 1960.² A comparison of carbonyl IR spectra and x-ray powder patterns indicated that this compound is isostructural with $\text{Co}_4(\text{CO})_{12}$ and thus has C_{3v} symmetry.³ Mays^{4,5} and coworkers have carried out IR and mass spectra on this compound and kinetic isotope studies on the protonation of the anion $\text{FeCo}_3(\text{CO})_{12}^-$, and proposed on the basis of this evidence that the hydrogen atom might be located in the center of the cluster.

White and Wright⁶ confirmed the C_{3v} symmetry of the molecule through inelastic neutron scattering spectroscopy, and on the basis of the magnitude of bonding force constants also concluded that the hydrogen atom must be located in the center of the cluster and not outside of the tetrahedron. Following earlier success in our laboratory in the characterization and elucidation of the intramolecular tautomerism of hydrogen through ¹H NMR studies of $\text{P}(\text{OCH}_3)_3$ -substituted hydro-

rido-metal cluster complexes,⁷ we were prompted to synthesize the series of complexes described in the title. A parallel but independent effort by Cooke and Mays on a more extensive but nonoverlapping series of complexes with a variety of phosphorus donor ligands has recently been described in the literature.⁸ The infrared and Mössbauer data obtained in both studies yielded some useful information about stereochemistry; however, this could not lead to a conclusive assignment for the position of hydrogen on the cluster. Significantly, in every case, no ¹H NMR signal for this hydrogen atom could be obtained. We then turned to a low-temperature x-ray study on the tris(trimethyl phosphite) derivative in an attempt to locate the hydrogen atom. The full account of this work is contained in the present article. A complementary and independent neutron diffraction study of $\text{HFeCo}_3(\text{CO})_9[\text{P}(\text{OCH}_3)_3]_3$ appears in a companion paper.⁹

Experimental Section

Reagents. $\text{Co}_2(\text{CO})_8$ was purchased from Ventron Chemical Co., $\text{Fe}(\text{CO})_5$ from Strem Chemical Co., and $\text{P}(\text{OCH}_3)_3$ from Matheson

Table I. Carbonyl Absorptions in the IR and Mössbauer^a Parameters

Compd	$\nu(\text{CO})$ IR, cm^{-1b}	Chemical isomer shift ^c δ , mm/s	Quadrupole split Δ , mm/s	Full width at half-maximum Γ , mm/s
II				
$\text{FeCo}_3(\text{CO})_{12}^-$	2066 w, 2008 s, 1974 m, 1932 m, 1815 m	-0.136	0	0.586
I				
$\text{HFeCo}_3(\text{CO})_{12}$	2059 s, 2049 s, 2027 m, 1989 m, 1886 s	-0.046	0	0.298
III				
$\text{HFeCo}_3(\text{CO})_{11}\text{P}(\text{OCH}_3)_3$	2080 m, 2046 s, 2038 vs, 2015 s, 2004 w, 1975 m, 1898 w, 1871 m, 1856 m	0.055	0.373	0.334
IV				
$\text{HFeCo}_3(\text{CO})_{10}[\text{P}(\text{OCH}_3)_3]_2$	2070 sh, 2062 m, 2032 s, 2024 s, 2002 s, 1964 m, 1886 w, 1849 m, 1833 m, 1816 w	0.043	0.239	0.362
V				
$\text{HFeCo}_3(\text{CO})_9[\text{P}(\text{OCH}_3)_3]_3$	2040 s, 2009 m, 1990 s, 1963 w, 1833 m, 1821 m	-0.066	0	0.348
VI				
$\text{HFeCo}_3(\text{CO})_8[\text{P}(\text{OCH}_3)_3]_4$	2043 w, 2022 w, 2012 m, 1985 m, br, 1945 m, 1827 w, 1816 m	-0.031	0.230	0.322

^a Mössbauer parameters are listed only for the principal absorptions associated with the indicated species. Minor components or impurity peaks as evident in supplementary Figures D and G are discussed in the text. ^b Cyclohexane solution except for II (acetonitrile) and VI (CCl_4); see supplementary Figures A–C. ^c Relative to Fe/Pd standard. Estimated errors 0.01 mm/s.

Coleman and Bell. These were used as purchased with no further purification needed. $\text{HFeCo}_3(\text{CO})_{12}$ (I) and $[\text{FeCo}_3(\text{CO})_{12}]^-$ (II) were prepared from $\text{Fe}(\text{CO})_5$ and $\text{Co}_2(\text{CO})_8$ by the method of Chini et al.² All other reagents and solvents were those available from most chemical vendors. Syntheses were carried out under an inert N_2 atmosphere (purified over a copper catalyst) using Schlenk techniques. Compounds thus prepared were stored under N_2 or vacuum; however, chromatography and other manipulations were done in the air after it was found that the compounds were air stable over periods of a few hours.

IR Spectra. All carbonyl region IR spectra were obtained on a Beckman IR-4 spectrophotometer equipped with a LiF prism. Solution spectra were obtained in CaF_2 cells and were calibrated against a sharp cyclohexane absorption at 4.676μ . A summary of the carbonyl absorptions of the compounds utilized or isolated for the first time in this work is given in Table I.

NMR Spectra. All spectra presented here were obtained on a Varian A-60D using dichloromethane as solvent and Me_4Si as internal reference. Attempts to locate the hydride resonance were made on both the A-60D and a Varian HA-100 using a variety of solvents and temperatures but were unsuccessful.

Mössbauer Spectra. Mössbauer spectra were recorded at 80 K employing a moving-source stationary sample technique. These spectra were analyzed using curve-fitting and calibration programs written by Dr. W. Dollase of the UCLA Geology Department.¹⁰ These programs resolve the observed spectra into their component peaks and determine their parameters by comparison with those of known compounds. Mössbauer parameters are summarized in Table I.

Mass Spectra. All mass spectra were obtained on an AE1-MS9 spectrometer using an ionizing voltage of 70 eV and probe temperature of 100–150 °C. The MASPAN computer program written by Mark Andrews of this department¹¹ was used to calculate hydrogen atom loss and to verify the observed isotopic multiplets. Mass spectral parameters are summarized in supplementary tables A–E.⁴⁷

Elemental Analyses. C and H were determined by Ms. Heather King of this department.

Reactions of $\text{HFeCo}_3(\text{CO})_{12}$ (I) with $\text{P}(\text{OMe})_3$. **1. Ratio of $\text{P}(\text{OCH}_3)_3$:I 1.5:1.** $\text{P}(\text{OMe})_3$ (0.663 g, 5.35 mmol) and I (2.03 g, 3.56 mmol) were dissolved in 400 mL of hexane and heated at reflux for 3 h. The dark purple solution was concentrated and chromatographed on a silica gel column prepared in hexane. With dichloromethane–hexane (10:90) solvent mixture a purple band of $\text{HFeCo}_3(\text{CO})_{11}\text{P}(\text{OMe})_3$ (III, 1.13 g, 1.70 mmol, 48%) is eluted: $^1\text{H NMR}$ τ 6.33 (doublet, $\text{P}(\text{OCH}_3)_3$), $J(^{31}\text{P}-\text{H}) = 11.5$ Hz.

Anal. Calcd for $\text{C}_{14}\text{H}_{10}\text{Co}_3\text{FeO}_{14}\text{P}$: C, 25.25; H, 1.51. Found: C, 24.45; H, 1.74.

When the dichloromethane–hexane ratio is increased to 30:70 a brown band and another purple band develop. The brown band was identified by IR spectroscopy as $\text{Fe}(\text{CO})_3[\text{P}(\text{OMe})_3]_2$ ¹² (75.5 mg,

0.195 mmol, 5.5%). The purple band eluted cleanly and consisted of $\text{HFeCo}_3(\text{CO})_{10}[\text{P}(\text{OMe})_3]_2$ (IV, 0.89 g, 1.16 mmol, 33%): $^1\text{H NMR}$ τ 6.33 (doublet, $\text{P}(\text{OCH}_3)_3$), $J(^{31}\text{P}-\text{H}) = 11.3$ Hz.

Anal. Calcd for $\text{C}_{16}\text{H}_{19}\text{Co}_3\text{FeO}_{16}\text{P}_2$: C, 25.22; H, 2.51. Found: C, 25.15; H, 2.49.

When the dichloromethane–hexane ratio is further increased to 50:50, a small quantity of the purple compound $\text{HFeCo}_3(\text{CO})_9[\text{P}(\text{OMe})_3]_3$ (V, 17.0 mg, 0.02 mmol, 0.6%) is eluted: $^1\text{H NMR}$ τ 6.31 (doublet, $\text{P}(\text{OCH}_3)_3$), $J(^{31}\text{P}-\text{H}) = 11.0$ Hz.

Anal. Calcd for $\text{C}_{18}\text{H}_{28}\text{Co}_3\text{FeO}_{18}\text{P}_3$: C, 25.20; H, 3.29. Found: C, 24.94; H, 3.22.

The overall reaction yield of isolated, identified compounds was 87% (based on I).

2. Ratio of $\text{P}(\text{OMe})_3$:I 3.6:1. $\text{P}(\text{OMe})_3$ (1.58 g, 12.7 mmol) and I (2.01 g, 3.52 mmol) were dissolved in 400 mL of hexane and heated at reflux for 4 h. After concentration, the dark purple solution was chromatographed as before. Under elution with dichloromethane–hexane (20:80) a small amount of brown material, $\text{Fe}(\text{CO})_3[\text{P}(\text{OMe})_3]_2$ (12.1 mg, 0.031 mmol, 0.9%) was removed. Further elution with dichloromethane–hexane (50:50) yielded the purple compound V (2.10 g, 2.44 mmol, 69%).

With a much higher ratio of dichloromethane–hexane (80:20) yet another purple band eluted very slowly. This band consisted of $\text{HFeCo}_3(\text{CO})_8[\text{P}(\text{OMe})_3]_4$ (VI, 0.12 g, 0.13 mmol, 3.8%): $^1\text{H NMR}$ τ 6.35 (doublet, rel intensity 3, $J(^{31}\text{P}-\text{H}) = 10.8$ Hz) and 6.39 (doublet, rel intensity 1, $J(^{31}\text{P}-\text{H}) = 8.8$ Hz). Both peaks are attributed to $\text{P}(\text{OCH}_3)_3$.

Anal. Calcd for $\text{C}_{20}\text{H}_{37}\text{Co}_3\text{FeO}_{20}\text{P}_4$: C, 25.18; H, 3.91. Found: C, 24.97; H, 3.8.

The reaction yield of isolated products was 74%.

3. Ratio of $\text{P}(\text{OMe})_3$:I 4.8:1. In an attempt to maximize the yield of VI, $\text{P}(\text{OMe})_3$ (1.26 g, 10.8 mmol) and I (1.20 g, 2.1 mmol) were dissolved in 400 mL of hexane and heated at reflux for 24 h. A large amount of solid material was observed in the reaction flask. After concentration, the dark purple solution was chromatographed as before. Brown material eluted early but was not collected; V (212.7 mg, 0.248 mmol, 11.8%) followed; and, finally, elution with dichloromethane–hexane (80:20) yielded VI (0.27 g, 0.28 mmol, 13%).

Discussion

Treatment of $\text{HFeCo}_3(\text{CO})_{12}$ (I) with trimethyl phosphite yields the series of compounds $\text{HFeCo}_3(\text{CO})_{12-x}[\text{P}(\text{OMe})_3]_x$ ($x = 1-4$), III–VI. The yields of the various derivatives can be maximized by varying the amount of added phosphite, except that the yield of VI is limited by its thermal instability.

Mass Spectra. All five neutral compounds, I and III–VI, give parent ions corresponding to their formulations as indicated in supplemental tables A, C, E, F, and G. In addition, peaks

Table II. Crystal Data, Space Group $P2_1/c$

	-139 °C	25 °C
Z	4	4
a, Å	15.992 (6) ^a	16.336 (3)
b, Å	10.638 (3)	10.896 (2)
c, Å	18.403 (4)	18.583 (2)
β , deg	98.515 (25)	97.259 (12)
V, Å ³	3093 (3)	3281 (1)
$d_{\text{calcd.}}$, g cm ⁻³	1.843 (2)	1.737 (1)
$d_{\text{exp.}}$, g cm ⁻³		1.72 (1)

^a The numbers given in parentheses here and in succeeding tables are the estimated standard deviations in the least significant digit.

^b Measured by flotation in $\text{C}_2\text{H}_4\text{Br}_2$ and CCl_4 .

arising from loss of CO groups from each compound are observed, up to and including a peak corresponding to $\text{HFeCo}_3[\text{P}(\text{OMe})_3]_x$ ($x = 0-4$) for each compound. For VI, peaks corresponding to V are also observed, presumably due to decomposition on the probe.

For $\text{HFeCo}_3(\text{CO})_{12}$ (I), we confirm that little hydrogen loss occurs in the ionization and fragmentation multiplets, as reported earlier.⁴ Even less hydrogen loss is observed in the phosphite-substituted clusters. Three of the observed multiplets have been subjected to computer analysis using MASPAN:¹¹ the parent ion and the bare metal cluster ion multiplets in the mass spectrum of II and the monophosphito metal cluster ion multiplet in the spectrum of III. The observed and calculated peak heights in these multiplets are presented in supplementary tables B and D. *R* factors are in the range of 10-20%, indicating a likely but not necessarily certain assignment: 8% hydrogen loss is observed in the parent ion peak for HFe

$\text{Co}_3(\text{CO})_{12}$, rising to 22% hydrogen loss in the bare metal cluster multiplet, HFeCo_3 , of this spectrum. A significant reduction in hydrogen loss, namely, 7%, is observed for the corresponding phosphite-substituted metal cluster multiplet, $\text{HFeCo}_3\text{P}(\text{OCH}_3)_3$, in the spectrum of III.

Infrared Spectra. Band maxima of the carbonyl absorptions of the new derivatives synthesized in this work, III-VI, together with the previous known I and II for calibration and comparison are given in Table I. The spectral tracings for each of these are given as supplementary Figures D, E, and F.⁴⁷ An analysis of the carbonyl stretching region for I has appeared.¹³ The positions of the principal absorptions in our work agree within 1 cm⁻¹ of those reported.

Substitution of CO by $\text{P}(\text{OMe})_3$ produces both a decrease in symmetry and a shift of the bands to lower frequencies. The carbonyl stretching absorptions for the trisubstituted derivative, V, are considerably simpler than for the mono- and disubstituted derivatives III and IV, indicating a higher symmetry and/or the presence of only one isomer for V. In the terminal carbonyl stretching region, three principal absorptions are noted for V, one fewer than in the parent cluster I, although one of these, at 1990 cm⁻¹ for V, is quite broad. A high symmetry in the environment of the iron atom in V is indicated by the Mössbauer data and a molecular C_{3v} symmetry has been found in the structure study, both described below.

For the tetrasubstituted derivative, VI, a lower symmetry is again indicated. The fourth substitution could be either on iron or cobalt, though the latter choice seems unlikely, given the general observation that in metal clusters each metal tends to become substituted by at least one ligand in preference to multiple substitutions on any one metal.¹⁴ The small effect of substitution by the fourth $\text{P}(\text{OMe})_3$ ligand on the bridging

Table III. Atomic Positional Parameters

Atom	x	y	z
Co1	0.348 25 (5)	0.071 15 (7)	0.236 45 (4)
Co2	0.193 92 (5)	0.115 11 (7)	0.230 80 (4)
Co3	0.248 74 (5)	-0.100 17 (7)	0.257 57 (4)
Fe	0.282 95 (5)	0.070 36 (7)	0.355 47 (4)
P1	0.407 17 (9)	0.058 12 (13)	0.137 51 (7)
P2	0.105 34 (9)	0.169 09 (13)	0.134 70 (7)
P3	0.215 48 (10)	-0.232 86 (13)	0.168 27 (7)
O1	0.4893 (3)	0.1772 (5)	0.3357 (2)
O2	0.1101 (3)	0.2823 (5)	0.3209 (3)
O3	0.2539 (3)	-0.2696 (4)	0.3812 (2)
O4	0.2980 (3)	0.3362 (4)	0.2104 (2)
O5	0.0719 (3)	-0.0647 (4)	0.2778 (2)
O6	0.4287 (3)	-0.1717 (4)	0.2806 (2)
O7	0.1537 (3)	0.0278 (5)	0.4505 (2)
O8	0.4155 (3)	-0.0561 (5)	0.4578 (2)
O9	0.3222 (3)	0.3290 (4)	0.4060 (2)
O11 ^a	0.5078 (3)	0.0683 (4)	0.1429 (2)
O12	0.3828 (3)	0.1567 (4)	0.0721 (2)
O13	0.3808 (3)	-0.0699 (4)	0.0968 (2)
O21	0.0076 (3)	0.1369 (4)	0.1349 (2)
O22	0.1023 (3)	0.3180 (4)	0.1309 (2)
O23	0.1104 (3)	0.1228 (4)	0.0524 (2)
O31	0.2908 (3)	-0.3281 (4)	0.1633 (2)
O32	0.1923 (3)	-0.1699 (4)	0.0900 (2)
O33	0.1332 (3)	-0.3189 (4)	0.1665 (2)
C1	0.4327 (4)	0.1353 (5)	0.2978 (3)
C2	0.1458 (4)	0.2150 (6)	0.2879 (3)
C3	0.2518 (4)	-0.2008 (6)	0.3332 (3)
C4	0.2859 (4)	0.2298 (5)	0.2183 (3)
C5	0.1368 (4)	-0.0351 (5)	0.2609 (3)
C6	0.3722 (4)	-0.1039 (5)	0.2652 (3)
C7	0.2032 (4)	0.0434 (5)	0.4123 (3)
C8	0.2654 (4)	-0.0079 (6)	0.4168 (3)
C9	0.3073 (4)	0.2287 (6)	0.3858 (3)
H	0.267 (7)	0.023 (11)	0.200 (6)

^a Methoxy groups are numbered to correspond to the phosphorus atom to which they are attached.

Table IV. Atomic Thermal Parameters ($\times 10^4$)

Atom	β_{11}^a	β_{22}	β_{33}	β_{12}	β_{13}	β_{23}
Co1	15.0 (3)	24.1 (6)	5.5 (2)	0.2 (3)	3.2 (2)	0.2 (3)
Co2	15.4 (3)	23.2 (6)	5.5 (2)	2.3 (3)	2.2 (2)	-0.1 (3)
Co3	16.4 (3)	21.2 (6)	5.2 (2)	0.1 (3)	2.7 (2)	-0.4 (3)
Fe	17.5 (3)	28.9 (6)	4.7 (2)	1.1 (4)	2.6 (2)	-1.8 (3)
P1	15.5 (5)	27.4 (11)	6.1 (3)	-1.2 (6)	3.1 (3)	-3.9 (5)
P2	15.6 (6)	26.9 (11)	6.5 (4)	-1.0 (6)	1.4 (4)	0.2 (5)
P3	19.4 (6)	23.3 (11)	6.8 (3)	-1.3 (7)	2.9 (4)	-2.2 (5)
O1	24 (2)	74 (5)	14 (1)	-12 (3)	3 (1)	-7 (2)
O2	41 (3)	77 (5)	16 (1)	28 (3)	5 (2)	-11 (2)
O3	48 (3)	56 (4)	14 (1)	-6 (3)	4 (2)	15 (2)
O4	25 (2)	32 (4)	19 (1)	-3 (2)	1 (1)	5 (2)
O5	21 (2)	47 (4)	16 (1)	-1 (2)	7 (1)	2 (2)
O6	22 (2)	41 (4)	17 (1)	5 (2)	5 (1)	3 (2)
O7	32 (2)	74 (5)	13 (1)	-4 (3)	11 (1)	2 (2)
O8	29 (2)	72 (5)	12 (1)	14 (3)	-1 (1)	-1 (2)
O9	41 (2)	42 (4)	14 (1)	-6 (2)	8 (1)	-6 (2)
O11	14 (2)	55 (4)	12 (1)	1 (2)	3 (1)	0 (2)
O12	23 (2)	46 (4)	8 (1)	-6 (2)	4 (1)	5 (2)
O13	30 (2)	33 (3)	10 (1)	-6 (2)	10 (1)	5 (2)
O21	18 (2)	35 (3)	12 (1)	-4 (2)	4 (1)	-6 (2)
O22	19 (2)	32 (3)	11 (1)	-1 (2)	-2 (1)	1 (2)
O23	18 (2)	55 (4)	8 (1)	-3 (2)	3 (1)	-2 (2)
O31	33 (2)	40 (4)	11 (1)	8 (2)	2 (1)	-8 (2)
O32	35 (2)	38 (4)	8 (1)	-2 (2)	-2 (1)	1 (2)
O33	33 (2)	62 (4)	15 (1)	-19 (3)	9 (1)	-7 (2)
C1	14 (2)	44 (5)	10 (2)	2 (3)	4 (1)	2 (2)
C2	26 (3)	37 (5)	11 (2)	6 (3)	3 (2)	0 (2)
C3	19 (2)	38 (6)	14 (2)	-3 (3)	4 (2)	-2 (2)
C4	21 (2)	36 (5)	7 (1)	3 (3)	1 (1)	-1 (2)
C5	24 (3)	33 (5)	6 (1)	3 (3)	2 (2)	2 (2)
C6	19 (2)	30 (4)	6 (1)	-3 (3)	3 (1)	1 (2)
C7	21 (2)	39 (5)	7 (1)	1 (3)	1 (1)	1 (2)
C8	22 (2)	48 (5)	8 (1)	-1 (3)	5 (2)	-5 (2)
C9	26 (3)	40 (5)	6 (1)	8 (3)	4 (2)	2 (2)

^a The expression for the anisotropic temperature factor is of the form $\exp[-(\beta_{11}h^2 + \beta_{22}k^2 + \beta_{33}l^2 + 2\beta_{12}hk + 2\beta_{13}hl + 2\beta_{23}kl)]$.

Table V. Group Parameters

Group	x	y	z	ϕ^a	θ	ρ	$B, \text{\AA}^2$
M11 ^b	0.5670 (4)	0.0105 (6)	0.1996 (3)	-2.96 (7)	2.37 (6)	2.07 (8)	2.13 (10)
M12	0.4175 (4)	0.2807 (6)	0.0758 (4)	1.24 (6)	-2.80 (5)	-0.02 (6)	2.35 (11)
M13	0.4106 (5)	-0.1067 (7)	0.0294 (4)	1.57 (6)	2.67 (6)	-1.81 (7)	2.64 (12)
M21	-0.0247 (4)	0.0132 (6)	0.1159 (3)	1.08 (7)	2.50 (5)	-2.88 (7)	2.00 (10)
M22	0.0403 (4)	0.3839 (6)	0.0790 (3)	2.67 (5)	2.87 (5)	-0.75 (6)	1.93 (10)
M23	0.1905 (4)	0.1303 (6)	0.0246 (3)	0.36 (6)	2.70 (5)	-0.61 (7)	2.13 (10)
M31	0.2928 (4)	-0.4148 (6)	0.1039 (4)	-1.09 (6)	2.96 (6)	-0.81 (6)	2.49 (11)
M32	0.1322 (4)	-0.2179 (6)	0.0296 (4)	-1.99 (6)	2.75 (6)	-1.02 (6)	2.50 (11)
M33	0.1219 (5)	-0.3931 (7)	0.2288 (4)	3.33 (7)	2.49 (7)	1.07 (8)	3.34 (14)

^a The definitions of these parameters are given in ref. 29. ^b Methyl group.

carbonyls around the cobalt face, relative to the effects of substitution of the first three P(OMe)₃ ligands on these modes, is consistent with substitution of the fourth ligand on iron. This sequence of substitution is further supported by the ¹H NMR data, discussed below.

NMR Spectra. The ¹H resonances due to P(OMe)₃ are indicated in the Experimental Section. Those for III, IV, and V are quite simple. Each consists of a sharp doublet, with little difference in chemical shifts or ¹³P-H coupling constants. The spectrum of VI, by contrast, shows two poorly resolved doublets (see Experimental Section). This is consistent with substitution at each of the three cobalt atoms (equivalent) and the iron atom (unique). The observations support the order of substitution given above.

Several attempts were made to observe the resonance due to the metal hydride, both on the A-60D and HA-100 instruments. Various solvents (e.g., benzene, acetonitrile, etc.) and

temperatures (-100 to 60 °C) were used. In addition, Cr-(acac)₃ was employed in hope of enhancing relaxation processes. However, no signal due to hydrogen on the metal cluster was observed.

Mössbauer Spectra. The Mössbauer spectra of compounds I-VI were obtained and have been presented in Table I. The spectra are shown in supplementary Figures D, E, and F. Doublets marked a, b, and c in the spectra of II, I, and III, respectively, are not included in Table I. These may be attributed as follows: peak a (δ 0.77 and Δ = 0.28 mm/s) is very likely due to a cationic species such as [Fe(acetone)₆]²⁺ which might be produced by disproportionation of the Fe(CO)₅ employed in the original preparation.¹⁵ Parameters of peaks b and c are δ 0.15, Δ = 0.87 and δ 0.15, Δ = 0.92 mm/s; no further information regarding these minor constituents was sought. The large width observed for compound II may be due to the presence of cationic impurities which distort the elec-

Table VI. Derived Parameters for Group Atoms

Group	Atom	x	y	z
M11	C11	0.5670	0.0105	0.1996
	H1	0.5797	0.0565	0.2473
	H2	0.5432	-0.0742	0.2083
	H3	0.6202	0.0002	0.1777
M12	C12	0.4175	0.2807	0.0758
	H1	0.4737	0.2832	0.0582
	H2	0.3757	0.3312	0.0419
M13	H3	0.4230	0.3168	0.1265
	C13	0.4106	-0.1067	0.0294
	H1	0.4736	-0.1145	0.0372
M21	H2	0.3849	-0.1887	0.0112
	H3	0.3930	-0.0396	-0.0078
	C21	-0.0247	0.0132	0.1159
M22	H1	0.0149	-0.0495	0.1429
	H2	-0.0817	0.0042	0.1314
	H3	-0.0293	-0.0023	0.0618
	C22	0.0403	0.3839	0.0790
M23	H1	0.0547	0.4754	0.0810
	H2	0.0426	0.3513	0.0283
	H3	-0.0179	0.3718	0.0915
	C23	0.1905	0.1303	0.0246
M31	H1	0.2291	0.0571	0.0373
	H2	0.1689	0.1291	-0.0293
	H3	0.2222	0.2102	0.0374
	C31	0.2928	-0.4148	0.1039
M32	H1	0.2452	-0.4765	0.1004
	H2	0.2915	-0.3712	0.0556
	H3	0.3478	-0.4602	0.1166
	C32	0.1322	-0.2179	0.0296
M33	H1	0.0728	-0.1951	0.0351
	H2	0.1469	-0.1793	-0.0164
	H3	0.1373	-0.3114	0.0268
	C33	0.1219	-0.3931	0.2288
M33	H1	0.1128	-0.3428	0.2728
	H2	0.0684	-0.4376	0.2088
	H3	0.1677	-0.4562	0.2432

tronic field gradient around the $\text{FeCo}_3(\text{CO})_{12}^-$ anion. The important information which can be extracted from the isomer-shift data is a small increase in isomer shift upon protonation II to I indicating a small decrease in s-electron density, consistent with the trends observed for both polynuclear and mononuclear iron complexes.¹⁶ This effect is identical with that observed by Cooke and Mays.⁸ The lack of resolvable quadrupole splitting in II, I, and V is consistent with C_{3v} symmetry in these species; the splitting observed in the other compounds indicates lowered symmetry and the small magnitude indicates that the iron atom has a nearly octahedral environment.¹⁷

The small quadrupole splitting reported by Cooke and Mays⁸ for I, II, and the trisubstituted derivatives $\text{HFeCo}_3(\text{CO})_9[\text{PMePh}_2]_3$ and $\text{HFeCo}_3(\text{CO})_9(\text{dppe})_2$ (dppe = diphos = bisdiphenylphosphinoethane) are too small to be uniquely determined without placing unreasonable constraints on line width and shape.¹⁰ We chose not to add such constraints and to report the peaks for I, II, and V as singlets (see Table I and supplementary Figures D and F). The quadrupole splitting observed for III and IV are consistent with a distortion of the C_{3v} symmetry resulting from substitution at Co, and is equivalent to that observed by Cooke and Mays⁸ in their analogous derivatives. The small quadrupole splitting for VI indicates only a small distortion accompanying substitution of CO by $\text{P}(\text{OCH}_3)_3$ at iron. This is to be contrasted with the larger splitting (1.01 mm/s) observed by Cooke and Mays⁸ for isomer B of $\text{HFeCo}_3(\text{CO})_8(\text{dppe})_2$. In the latter compound the bridging ligand undoubtedly causes some significant distortion in the environment of the iron and hence the difference in the quadrupole splitting.

Unfortunately, although the spectroscopic studies yielded

valuable information concerning the disposition of the ligands about the iron tricobalt cluster, none of this gave direct information about the position of the hydride atom (terminal, central, or face bridging). In order to answer this question, a crystal structure determination was undertaken. All five compounds gave promising crystals except that those of I proved to be unstable in the x-ray beam. V was chosen because it seemed to possess a higher symmetry, thus minimizing possible distortions of bond lengths and angles.

Crystallographic Study

Suitable crystals of $\text{HFeCo}_3(\text{CO})_9[\text{P}(\text{OCH}_3)_3]_3$ (V) prepared as described above were recrystallized from a dichloromethane-hexane solution. The solution was filtered and put in a Schlenk tube. Solvent was removed until small crystals began to form. The solution was then heated to dissolve those crystals and the Schlenk tube was sealed under nitrogen and immersed in a Dewar flask of hot salt water. The flask was wrapped in cheesecloth and placed in the low-temperature compartment of a refrigerator at -20°C overnight. The crystals are small, well-formed, purple-black polyhedra and hexagonal platelets.

Crystallographic Data. Preliminary x-ray diffraction photographs indicated monoclinic symmetry. Weissenberg photographs had systematic absences for reflections $h0l$, $l = 2n + 1$. In addition, diffractometer data showed absences for reflections $0k0$, $k = 2n + 1$, indicative of space group $P2_1/c$.¹⁸

The crystal used for data collection was a fragment bounded by $\{001\}$, $\{100\}$, $\{110\}$, and $\{1\bar{1}0\}$. Crystal dimensions normal to these faces from a point in the center of the crystal were 0.125, 0.125, 0.166, and 0.166 mm, respectively. The crystal was sealed under nitrogen in a capillary and mounted with c approximately along the ϕ axis of a

Table VII. Bond Lengths (Å)

Bond	Distance	Bond	Distance
Fe-Co1	2.562 (1)	C7-O7	1.145 (7)
Fe-Co2	2.559 (1)	C8-O8	1.138 (7)
Fe-Co3	2.558 (1)	C9-O9	1.142 (7)
Average	2.560 ± 0.002 ^a	Average	1.142 ± 0.004
Co1-Co2	2.499 (1)	P1-O11	1.602 (4)
Co1-Co3	2.488 (1)	P1-O12	1.601 (4)
Co2-Co3	2.476 (1)	P1-O13	1.581 (4)
Average	2.488 ± 0.012	P2-O21	1.600 (4)
Co1-P1	2.175 (2)	P2-O22	1.586 (4)
Co2-P2	2.173 (2)	P2-O23	1.606 (4)
Co3-P3	2.172 (2)	P3-O31	1.586 (4)
Average	2.173 ± 0.002	P3-O32	1.582 (4)
Co1-C1	1.764 (6)	P3-O33	1.599 (5)
Co2-C2	1.751 (6)	Average	1.594 ± 0.010
Co3-C3	1.750 (6)	O11-C11	1.438 ^b
Average	1.755 ± 0.008	O12-C12	1.429
Co1-C4	1.964 (6)	O13-C13	1.447
Co1-C6	1.958 (6)	O21-C21	1.439
Co2-C4	1.950 (6)	O22-C22	1.450
Co2-C5	1.961 (6)	O23-C23	1.450
Co3-C5	1.929 (6)	O31-C31	1.435
Co3-C6	1.959 (6)	O32-C32	1.451
Average	1.954 ± 0.013	O33-C33	1.425
Fe-C7	1.788 (6)	Average	1.440 ± 0.010
Fe-C8	1.806 (6)	Co1-H	1.46 (11)
Fe-C9	1.800 (6)	Co2-H	1.68 (11)
Average	1.798 ± 0.009	Co3-H	1.74 (11)
C1-O1	1.148 (7)	Average	1.63 ± 0.15
C2-O2	1.145 (7)	H-Fe	2.88 (11)
C3-O3	1.144 (7)	H-C4	2.24 (12)
Average	1.146 ± 0.002	H-C5	2.58 (12)
C4-O4	1.161 (7)	H-C6	2.35 (12)
C5-O5	1.170 (7)	Average	2.39 ± 0.17
C5-O6	1.158 (7)	H-P1	2.70 (11)
Average	1.163 ± 0.006	H-P2	3.10 (11)
		H-P3	2.88 (11)
		Average	2.89 ± 0.20

^a The estimated errors of the average values are calculated using the formula $[\sum_{i=1}^n (x_i - \bar{x})^2 / (n - 1)]^{1/2}$ where x and \bar{x} are values and mean values, respectively. ^b No estimated standard deviations are given for distances involving atoms treated as members of rigid groups.

Syntex $P\bar{1}$ autodiffractometer equipped with a scintillation counter and a graphite monochromator. The crystal was then cooled to -139°C using the device constructed by Dr. C. E. Strouse of this department.¹⁹

Fifteen high-order reflections were centered in order to obtain accurate lattice parameters. After data collection was complete, the crystal was allowed to warm to room temperature and the above procedure was repeated to determine room temperature lattice parameters. The density of the crystals was measured by flotation in dibromomethane and carbon tetrachloride; crystal data are presented in Table II. Intensities were measured using the θ - 2θ scan technique with a scan rate of $2^\circ/\text{min}$ and a scan range from 1° below the $K\alpha_1$ peak to 1° above the $K\alpha_2$ peak. The takeoff angle was 4° and the ratio of background time to scan time was 1.0. The pulse height analyzer was set at an 85% window for Mo $K\alpha$ radiation.

The intensities of three standard reflections (7, 0, -6 ; 1, 1, 9; 1, 4, -7) were measured after each 97 intensity measurements. The standards showed little variation; the second reflection (1, 1, 9), with maximum variation, showed a drop in intensity of slightly less than 2σ or 6% during data collection. No correction for decay was made. The data was corrected for Lorentz and polarization effects²⁰ and processed as previously described.²¹ Of 9546 unique reflections (a quarter sphere) for which $2\theta \leq 60^\circ$, 6057 with $I \geq 3\sigma(I)$ were considered observed. A Wilson²² plot was used to put the data on an approximate absolute scale and normalized structure factors (E 's) were calculated.

Determination and Refinement of the Structure. Sign determination of 380 reflections with $E \geq 2.00$ was accomplished by use of the

program MULTAN.²³ The solution with the highest absolute figure of merit (ABS FOM = 1.1348)²⁴ and lowest residual (RESID = 18.37)²⁴ was chosen. The positions of four metal atoms and three phosphorus atoms were located on the E map²⁰ based on this solution.

Solution and early refinement were carried out using 3202 reflections with $2\theta \leq 45^\circ$. A Fourier summation based on the four metal positions (all considered to be Co atoms) and three phosphorus positions revealed positions of 17 oxygen and 15 carbon atoms. The positions of all 43 nonhydrogen atoms were located from a second electron density map.

Refinement was carried out by use of full-matrix least-squares procedures using atomic scattering factors for all nonhydrogen atoms compiled by Hanson et al.²⁵ Hydrogen atomic scattering factors were obtained from Stewart et al.²⁶ After two cycles of least-squares refinement²⁰ with all atoms assigned isotropic thermal parameters the discrepancy factors were $R_F = 0.091$ ²⁷ and $R_w = 0.108$ (all four metal atoms were assigned cobalt form factors). The isotropic thermal parameters of the four "cobalt" atoms were 0.98 (4), 0.99 (4), 0.97 (4), and 1.42 (4) \AA^2 . The metal atoms with $B = 1.42 \text{\AA}^2$ was assigned an iron form factor and its B value decreased to 1.0 \AA^2 . A cycle of refinement (all atoms isotropic) led to discrepancy factors $R_F = 0.091$ and $R_w = 0.107$ and thermal parameters 1.02 (4), 1.03 (4), and 1.01 (4) \AA^2 for the three cobalt atoms and 1.11 (4) \AA^2 for the iron atom.

Anomalous dispersion corrections²⁸ were applied to the form factors for Co, Fe, and P. Two cycles of refinement in which anisotropic thermal parameters for these seven heavy atoms were included led to

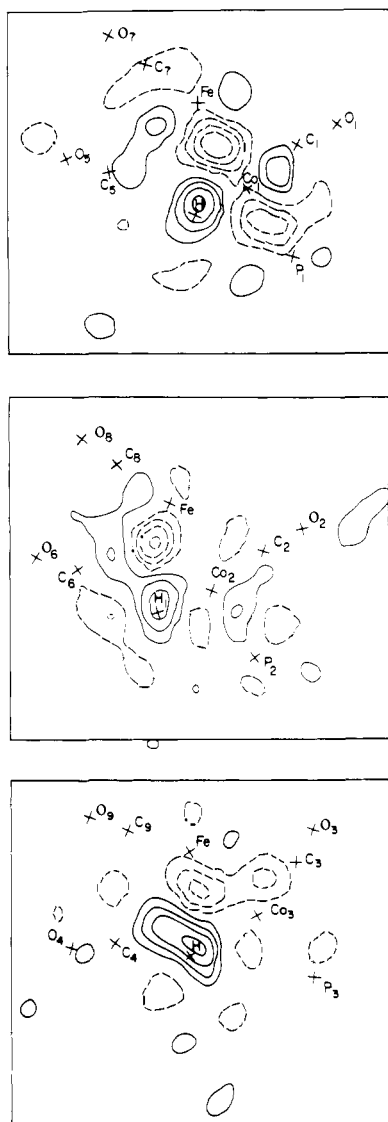


Figure 1. Difference Fourier maps using the 824 reflections with $\sin \theta/\lambda < 0.33$. Contours are drawn at 0.2, 0.4, 0.6, and $0.8 \text{ e } \text{\AA}^{-3}$ and dashed-line contours are drawn at $-0.2, -0.4, -0.6,$ and $-0.8 \text{ e } \text{\AA}^{-3}$. The positions of the hydride atom and of the atoms which define the least-squares plane are indicated; these correspond to least-squares planes B, C, and D of Table IX.

discrepancy factors $R_F = 0.069$ and $R_w = 0.086$. Careful examination of a Fourier map calculated at this point revealed the positions of most of the methyl hydrogen atoms. The methyl groups were treated as rigid groups^{20,29} ($C-H = 1.00 \text{ \AA}$, $H-C-H = 109.5^\circ$) in all subsequent refinement. Group isotropic thermal parameters were refined; carbon thermal parameters were set to be equal to the group parameters and each hydrogen thermal parameter was set at 1.0 \AA^2 greater than its group parameter.

The structure of the molecule at this stage ($R_F = 0.0644$ and $R_w = 0.0751$) shows near perfect C_{3v} symmetry (with the exception of the methoxy groups). However, the exact location of the hydrogen (terminal, central, or face-bridging) was still not determined.

A difference Fourier map was calculated from the full data set. This map shows a peak near the C_{3v} axis *outside* the cluster in a face-bridging position. Unfortunately this map contains many large peaks, although several of these are within 1 \AA of a metal atom. We then applied the method developed by Ibers and co-workers for $HRh(CO)(PPh_3)_3$ ³⁰ and $HMn_2(CO)_8PPh_2$ ³¹ and recently applied by Bau and co-workers to the structure of $H_3Mn_3(CO)_{12}$.³² Scattering due to hydrogen drops off rapidly with increasing $\sin \theta/\lambda$. Thus the hydrogen atom peaks should be enhanced when a difference Fourier map is calculated based on low-angle data.

Two additional difference Fourier maps were calculated, one using 1737 reflections ($\sin \theta/\lambda \leq 0.43$) and one using 824 reflections (\sin

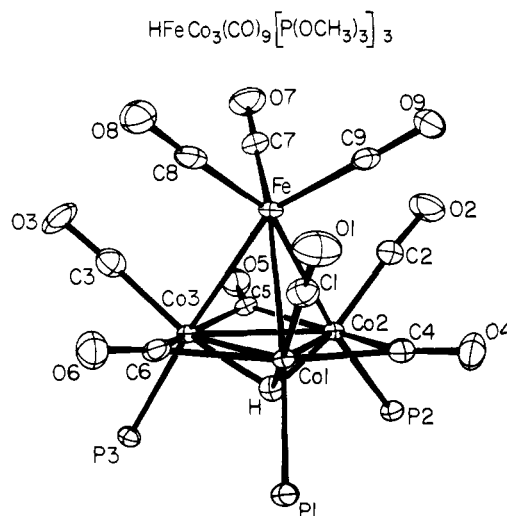


Figure 2. ORTEP plot of the $HFeCo_3(CO)_9[P(OCH_3)_3]_3$ molecule showing thermal ellipsoids at the 50% probability level. OCH_3 groups are omitted for clarity.

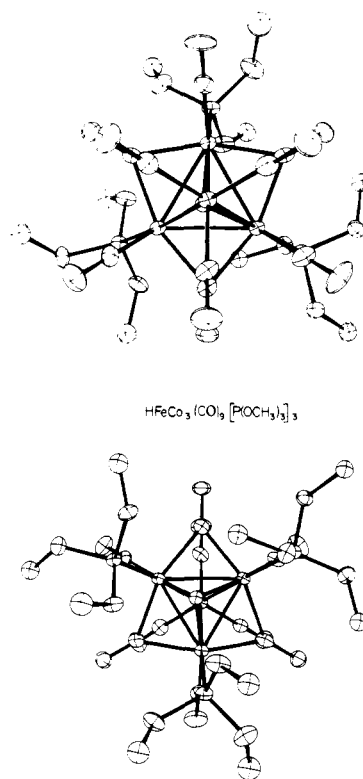


Figure 3. ORTEP plots of the $HFeCo_3(CO)_9[P(OCH_3)_3]_3$ molecule as viewed down the C_{3v} axis. Methyl hydrogen atoms are omitted for clarity. (a) Fe above, hydride below; (b) hydride above, Fe below.

$\theta/\lambda \leq 0.33$). On these maps the peak in the face-bridging position is very prominent, especially on the $\sin \theta/\lambda \leq 0.33$ map. The peak attributed to H has a maximum of $0.8 \text{ e } \text{\AA}^{-3}$. There are five peaks in the range $0.4-0.6 \text{ e } \text{\AA}^{-3}$; all lie within 1.1 \AA of a metal atom and are well removed from the C_3 axis. Therefore, the hydrogen atom was assigned the face-bridging position.

The hydrogen atom position was then refined based on the 824 inner sphere reflections. When the hydrogen atom is omitted from the structure factor calculations, $R_F = 0.0674$ and $R_w = 0.0807$. Addition of the hydrogen atom in a face-bridging position on the C_3 axis ($d(\text{Co}-H) = 1.53 \text{ \AA}$) outside the cluster reduced the discrepancy factors, $R_F = 0.0658$ and $R_w = 0.0788$. Refinement of position parameters of this hydrogen only (the isotropic temperature factor was

Table VIII. Bond Angles (deg)

Co1-Co2-Co3	60.01 (3)	Fe-Co1-C4	83.5 (2)
Co1-Co3-Co2	60.46 (4)	Fe-Co1-C6	81.6 (2)
Co2-Co1-Co3	59.52 (3)	Fe-Co2-C4	83.8 (2)
Average	60.00 ± 0.47	Fe-Co2-C5	79.4 (2)
Fe-Co1-Co2	60.74 (4)	Fe-Co3-C5	80.0 (2)
Fe-Co1-Co3	60.85 (3)	Fe-Co3-C6	81.7 (2)
Fe-Co2-Co3	61.05 (3)	Average	81.7 ± 1.8
Fe-Co2-Co1	60.86 (4)	Fe-Co1-H	87 (4)
Fe-Co3-Co1	61.02 (3)	Fe-Co2-H	83 (4)
Fe-Co3-Co2	61.09 (3)	Fe-Co3-H	82 (4)
Average	60.94 ± 0.14	Average	84 ± 3
Co1-Fe-Co2	58.41 (4)	P1-Co1-C4	100.6 (2)
Co1-Fe-Co3	58.13 (3)	P1-Co1-C6	94.2 (2)
Co2-Fe-Co3	57.86 (3)	P2-Co2-C4	98.7 (2)
Average	58.13 ± 0.28	P2-Co2-C5	99.8 (2)
Co1-Fe-C7	156.4 (2)	P3-Co3-C5	97.6 (2)
Co2-Fe-C8	154.6 (2)	P3-Co3-C6	99.9 (2)
Co3-Fe-C9	153.7 (2)	Average	90.5 ± 2.3
Average	154.9 ± 1.4	P1-Co1-C1	100.1 (2)
Co1-Fe-C8	100.6 (2)	P2-Co2-C2	92.1 (2)
Co1-Fe-C9	99.5 (2)	P3-Co3-C3	100.3 (2)
Co2-Fe-C7	101.8 (2)	Average	97.5 ± 4.7
Co2-Fe-C9	99.8 (2)	P1-Co1-H	94 (4)
Co3-Fe-C7	101.6 (2)	P2-Co2-H	106 (4)
Co3-Fe-C8	100.0 (2)	P3-Co3-H	94 (4)
Average	100.6 ± 1.0	Average	98 (4) ± 7
Fe-Co1-P1	175.82 (5)	C1-Co1-H	166 (4)
Fe-Co2-P2	171.04 (5)	C2-Co2-H	160 (4)
Fe-Co3-P3	175.30 (5)	C3-Co3-H	163 (4)
Average	174.05 ± 2.62	Average	163 ± 3
Fe-Co1-C1	79.9 (2)	C1-Co1-C4	95.6 (3)
Fe-Co2-C2	79.1 (2)	C1-Co1-C6	95.4 (2)
Fe-Co3-C3	84.0 (2)	C2-Co2-C4	95.6 (3)
Average	81.0 ± 2.6	C2-Co2-C5	93.5 (3)
		C3-Co3-C5	96.4 (3)
		C3-Co3-C6	91.2 (3)
		Average	94.6 ± 1.9
H-Co1-C4	80 (4)	Co1-P1-O11	120.0 (2)
H-Co1-C6	85 (4)	Co1-P1-O12	120.0 (2)
H-Co2-C4	76 (4)	Co1-P1-O13	109.5 (2)
H-Co2-C5	90 (4)	Co2-P2-O21	117.4 (2)
H-Co3-C5	89 (4)	Co2-P2-O22	108.2 (2)
H-Co3-C6	79 (4)	Co2-P2-O23	124.6 (2)
Average	83 ± 6	Co3-P3-O31	110.8 (2)
C4-Co1-C6	159.6 (2)	Co3-P3-O32	114.3 (2)
C4-Co2-C5	159.1 (2)	Co3-P3-O33	119.7 (2)
C5-Co3-C6	159.3 (2)	Average	116.1 ± 5.6
Average	159.3 ± 0.3	O11-P1-O12	97.7 (2)
Co1-C1-O1	177.5 (5)	O11-P1-O13	106.4 (2)
Co2-C2-O2	175.1 (6)	O12-P1-O13	100.9 (2)
Co3-C3-O3	177.9 (6)	O21-P2-O22	101.0 (2)
Fe-C7-O7	177.9 (5)	O21-P2-O23	97.0 (2)
Fe-C8-O8	177.1 (5)	O22-P2-O23	105.7 (2)
Fe-C9-O9	178.9 (5)	O31-P3-O32	107.2 (2)
Average	177.4 ± 1.3	O31-P3-O33	105.2 (3)
Co1-C4-O4	140.2 (5)	O32-P3-O33	98.2 (2)
Co2-C4-O4	140.1 (5)	Average	102.1 ± 4.0
Co2-C5-O5	139.7 (5)	P1-O11-C11	124.3
Co3-C5-O5	140.9 (5)	P1-O12-C12	121.3
Co1-C6-O6	140.6 (5)	P1-O13-C13	122.7
Co3-C6-O6	140.5 (5)	P2-O21-C21	120.8
Average	140.3 ± 0.4	P2-O22-C22	121.7
Co1-C4-Co2	79.4 (2)	P2-O23-C23	119.1
Co2-C5-Co3	79.1 (2)	P3-O31-C31	123.9
Co1-C6-Co3	78.9 (2)	P3-O32-C32	126.0
Average	79.1 ± 0.3	P3-O33-C33	120.2
Co1-H-Co2	105 (7)	Average	122.2 ± 2.2
Co1-H-Co3	102 (6)		
Co2-H-Co3	93 (6)		
Average	100 ± 6		

Table VIII (Continued)

Co1-H-Fe	63 (4)	Co2-Co1-C1	127.7 (2)
Co2-H-Fe	62 (3)	Co3-Co1-C1	129.0 (2)
Co3-H-Fe	62 (3)	Co1-Co2-C2	127.4 (2)
Average	62 ± 1	Co3-Co2-C2	128.1 (2)
Co2-Co1-C4	50.1 (2)	Co1-Co3-C3	129.0 (2)
Co3-Co1-C6	50.6 (2)	Co2-Co3-C3	133.7 (2)
Co1-Co2-C4	50.6 (2)	Average	129.2 ± 2.3
Co3-Co2-C5	49.9 (2)		
Co2-Co3-C5	51.0 (2)	Co2-Co1-C6	110.0 (2)
Co1-Co3-C6	50.5 (2)	Co3-Co1-C4	109.6 (2)
Average	50.4 ± 0.4	Co1-Co2-C5	109.5 (2)
C7-Fe-C8	94.5 (3)	Co3-Co2-C4	110.6 (2)
C7-Fe-C9	96.3 (3)	Co1-Co3-C5	111.1 (2)
C8-Fe-C9	97.6 (3)	Co2-Co3-C6	110.9 (2)
Average	96.1 ± 1.6	Average	110.3 ± 0.7
		P1-Co1-Co2	121.65 (6)
		P1-Co1-Co3	116.79 (5)
		P2-Co2-Co1	127.16 (5)
		P2-Co2-Co3	125.13 (5)
		P3-Co3-Co1	116.65 (5)
		P3-Co3-Co2	114.26 (5)
		Average	120.27 ± 5.18
		H-Co1-Co2	41 (4)
		H-Co1-Co3	43 (4)
		H-Co2-Co1	34 (4)
		H-Co2-Co3	44 (4)
		H-Co3-Co1	35 (4)
		H-Co3-Co2	43 (4)
		Average	40 ± 4

Table IX. Least-Squares Planes

Plane	Direction cosines ($\times 10^5$) with respect to			Description of plane
	<i>a</i>	<i>b</i>	<i>c</i> *	
A	-137	20 764	97 820	Co1, Co2, Co3
B	32 711	-91 832	22 289	Co1, Fe, P1, C1, C5 C7, O1, O5, O7
C	-65 971	-73 489	15 723	Co2, Fe, P2, C2, C6, C8, O2, O6, O8
D	98 427	-17 629	1131	Co3, Fe, P3, C3, C4 C9, O3, O4, O9
E	-508	18 899	98 197	Co1, Co2, C4
F	12 844	24 929	95 987	Co2, Co3, C5
G	-6295	26 026	96 349	Co1, Co3, C6

held constant) resulted in $R_F = 0.0658$ and $R_w = 0.0784$. One cycle of refinement with the larger data set ($2\theta \leq 45^\circ$) (hydrogen atom fixed, all others refined) led to discrepancy factors $R_F = 0.0637$ and $R_w = 0.0739$.

In order to assess the significance of the hydrogen atom location, a series of Hamilton^{33a} R ratio tests were carried out using the ratios $R_F = R_F/R'_F$ and $R_w = R_w/R'_w$, where the primed R factors are those with the hydrogen atoms included. For the small data set the ratios $R_F = 1.02$ and $R_w = 1.03$ are both much greater than that required for 99.5% significance (for three added parameters and $(n - m)^{33b}$ about 600, a ratio of 1.01 corresponds to 99.5% significance). With the larger data set the ratios are $R_F = 1.01$ and $R_w = 1.016$, again much greater than that required for 99.5% significance (for three added parameters and $(n - m)$ about 3000 a ratio of 1.002 corresponds to 99.5% significance).

At this point the data were corrected for the effects of absorption.²⁰ Transmission factors ranged from 0.7160 to 0.7899; an average correction of 0.7664 was applied to the unobserved reflections. Refinement using the corrected data ($2\theta < 45^\circ$), carried out without the hydrogen atom, converged with discrepancy factors $R_F = 0.061$ and $R_w = 0.071$. The hydrogen atom position was redetermined with this

absorption-corrected data set with similar results, both with respect to position found and the R ratio tests.

Further refinement for nonhydrogen atoms was carried out using all 6057 observed reflections (corrected for absorption); the CO_3 -face-bridging hydrogen position was refined using the 824 inner-sphere reflections. One cycle, with anisotropic thermal parameters for Co, Fe, and P and isotropic thermal parameters for the lighter atoms, led to discrepancy factors $R_F = 0.068$ and $R_w = 0.075$. Two cycles of refinement (with anisotropic thermal parameters for all nonhydrogen atoms except the methyl groups) converged with discrepancy factors $R_F = 0.061$ and $R_w = 0.068$. The hydrogen atom position was then refined (824 reflections) and a final cycle of refinement was carried out on the large data set. The final discrepancy factors are $R_F = 0.061$ and $R_w = 0.067$. Three sections of a difference map based on calculated structure factors which include all atoms except the hydride atom are shown in Figure 1; each section corresponds to a least-squares plane defined by the labeled atoms. There are the planes B, C and D which are also defined in Table IX.

The largest final shifts are as follows: group parameter, 0.22 σ ; nonhydrogen nongroup atom, 0.11 σ ; and hydrogen parameter 0.49 σ . The standard deviation of an observation of unit weight is 2.02.

A final three-dimensional difference Fourier map showed residuals in the range of -1.5 to $+2.4$ $e/\text{\AA}^3$; all peaks with $|\text{maxima}| > 1.0$ $e/\text{\AA}^3$ lie within 1.0 \AA of the metal and phosphorus atoms. A difference Fourier map based on the 824 low-angle reflections showed residuals in the range of -0.9 to $+0.7$ $e/\text{\AA}^3$; all with $|\text{maxima}| > 0.5$ $e/\text{\AA}^3$ lie close (< 1.2 \AA) to metal atoms.

The final least-squares parameters are given in Tables III-V. The parameters of the carbon and hydrogen atoms derived from the data in Table V are presented in Table VI. Structure factors calculated on the basis of the tabulated parameters are contained in supplementary Table H.

Description and Discussion of the Structure

The $HFeCO_3(CO)_9[P(OCH_3)_3]_3$ molecule, including the hydride atom, is shown in Figures 2 and 3. Bond distances and angles are given in Tables VII and VIII; average values, based

Table X

Planes	Angles	Interplanar Angles (deg)		Planes	Angles
		Planes	Angles		
A and B	88.5	A and E	1.1	B and C	60.4
A and C	89.9	A and F	7.9	B and D	60.9
A and D	91.5	A and G	4.7	C and D	58.8

Atom	Deviation of Atoms from Least-Squares Planes (Å) ^a			
	A	B	C	D
Co1	0*	-0.040*	-1.271	1.278
Co2	0*	-1.295	-0.012*	-1.220
Co3	0*	1.180	1.217	-0.019*
Fe	2.119	0.002*	-0.021*	-0.043*
P1	-1.792	0.082*	-2.251	2.475
P2	-1.590	-2.590	0.052*	-2.477
P3	-1.883	2.019	2.189	-0.073*
C1	1.233	-0.031*	-2.377	2.334
C2	1.239	-2.342	-0.020*	-2.306
C3	1.124	2.418	2.323	0.031*
C4	0.029	-1.974	-1.937	0.044*
C5	0.206	-0.031*	1.905	-1.912
C6	0.124	1.886	-0.021*	1.913
C7	3.073	0.029*	1.296	-1.388
C8	3.037	1.392	0.007*	1.249
C9	3.009	-1.321	-1.375	-0.031*
O1	1.999	-0.025*	-3.125	3.053
O2	1.976	-3.082	-0.015*	-3.076
O3	1.826	3.253	3.064	0.073*
O4	0.122	-2.975	-2.934	0.055*
O5	0.442	-0.028*	2.900	-2.920
O6	0.248	2.892	-0.015*	2.890
O7	3.720	0.043*	2.118	-2.232
O8	3.660	2.255	0.046*	2.027
O9	3.590	-2.159	-2.221	-0.036*
H	-0.751	-0.113	-0.206	0.177

^a An asterisk indicates atoms used to define respective planes.

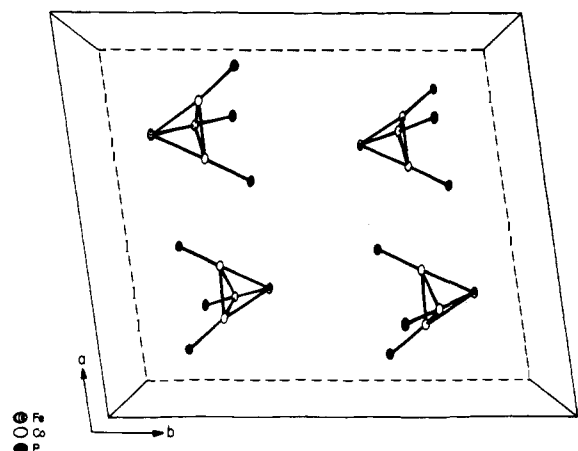


Figure 4. The packing arrangement of $\text{HFeCo}_3(\text{CO})_9[\text{P}(\text{OCH}_3)_3]_3$ molecules as viewed down the b axis of the unit cell. Carbon, hydrogen, and oxygen atoms are omitted.

on C_{3v} symmetry, are given for equivalent distances and angles. Least-squares plane data are given in Table IX; deviations from the more important of these are given in Table X.

Root-mean-square amplitudes of vibration along the three principal axes of the vibrational ellipsoids are given in Table XI; the smallest of these tend to be aligned with the C_{3v} axis of the molecule (see Figure 2). The packing in the unit cell is shown in Figure 4; the C_{3v} axis of the molecule aligns approximately with the c axis of the unit cell. As a consequence, the thermal expansion (from -139 to 25°C , see Table I) in the

c direction (0.98%) is much less than that in the a or b directions (2.15 and 2.43%, respectively).

Location of Hydrogen. We have confirmed, then, the proposed C_{3v} geometry but have shown that the hydride lies *outside* the cluster, in contrast to previous proposals; the metal-hydrogen distances are $\text{Co1-H} = 1.5$ (1), $\text{Co2-H} = 1.7$ (1), and $\text{Co3-H} = 1.7$ (1) Å and average to 1.63 ± 0.15 .³⁴ Since the asymmetry is not statistically significant we favor a symmetrically bridging C_{3v} structure. The neutron diffraction study yielded an average distance of 1.734 (7) Å⁹ in excellent agreement with our value bearing in mind that x-ray measurements derived from the scatter of electrons are often a little shorter than neutron diffraction values which locate the nucleus of the hydrogen atom.³⁵ The result is also in excellent agreement with the average Co-H distance of 1.67 (7) Å found in $\text{H}_4\text{Co}_4(\eta^5\text{-C}_5\text{H}_5)$,³⁶ a metal cluster containing hydrogen bridging each of the four tetrahedral faces. The hydride atom in the present structure is found to lie about 0.75 Å off the Co_3 plane (away from iron) also in excellent agreement for the analogous distance of 0.80 Å observed in $\text{H}_4\text{Co}_4(\eta^5\text{-C}_5\text{H}_5)$.³⁶ Face-bridging hydrogen has recently also been located in $\text{H}_4\text{Re}_4(\text{CO})_{12}$ ³⁷ and proposed but not located in $\text{H}_2\text{Ru}_6(\text{CO})_{18}$,³⁸ $[\text{HOs}_6(\text{CO})_{18}]^-$, and $\text{H}_2\text{Os}_6(\text{CO})_{18}$.³⁹ In $\text{H}_2\text{Ru}_6(\text{CO})_{18}$,³⁸ the face-bridging assignment for hydrogen was derived from the observed lengthening of the Ru-Ru bond by an average of 0.1 Å around two of the faces. In the present structure the average Co-Co distance around the Co_3 face is 2.488 (12) Å, not significantly different from 2.49 (2) Å, the average Co-Co distance in $\text{Co}_4(\text{CO})_{12}$.⁴⁰ The edges of the Co_3 face bridged by hydrogen in our structure are bridged by carbonyl groups. The presence of these additional bridging groups are expected to modify or even cancel any bond

Table XI. Root-Mean-Square Amplitudes of Vibration (\AA)^a

Atoms	Min	Median	Max
Co1	0.091 (2)	0.118 (1)	0.139 (1)
Co2	0.094 (2)	0.113 (2)	0.142 (1)
Co3	0.090 (2)	0.110 (2)	0.144 (1)
Fe	0.084 (2)	0.130 (1)	0.149 (1)
P1	0.096 (3)	0.124 (3)	0.142 (2)
P2	0.104 (3)	0.124 (3)	0.142 (2)
P3	0.099 (3)	0.120 (3)	0.157 (2)
O11	0.130 (7)	0.142 (7)	0.178 (6)
O12	0.101 (8)	0.157 (7)	0.182 (6)
O13	0.102 (8)	0.135 (7)	0.205 (6)
O21	0.121 (7)	0.139 (7)	0.171 (6)
O22	0.123 (8)	0.136 (7)	0.168 (7)
O23	0.112 (8)	0.148 (7)	0.181 (6)
O31	0.108 (8)	0.164 (7)	0.212 (6)
O32	0.110 (8)	0.147 (7)	0.218 (6)
O33	0.143 (7)	0.151 (8)	0.238 (7)
O1	0.143 (8)	0.162 (7)	0.221 (7)
O2	0.118 (9)	0.187 (7)	0.274 (7)
O3	0.110 (9)	0.205 (7)	0.250 (7)
O4	0.127 (8)	0.170 (7)	0.194 (7)
O5	0.137 (7)	0.165 (7)	0.180 (6)
O6	0.143 (8)	0.160 (7)	0.183 (7)
O7	0.121 (8)	0.204 (7)	0.214 (7)
O8	0.136 (8)	0.169 (7)	0.230 (7)
O9	0.132 (8)	0.163 (7)	0.230 (7)
C1	0.118 (10)	0.137 (10)	0.162 (9)
C2	0.132 (10)	0.142 (10)	0.187 (9)
C3	0.143 (10)	0.146 (10)	0.165 (10)
C4	0.110 (11)	0.140 (10)	0.167 (9)
C5	0.095 (12)	0.138 (9)	0.176 (9)
C6	0.095 (11)	0.130 (10)	0.157 (9)
C7	0.110 (11)	0.149 (10)	0.164 (9)
C8	0.105 (11)	0.165 (10)	0.173 (9)
C9	0.097 (12)	0.140 (10)	0.190 (9)

^a The equivalent B values are related to the root-mean-square amplitudes of vibration, $(\bar{U}^2)^{1/2}$, by the expression $B = 8\pi^2(\bar{U}^2)$.

lengthening effects that might have been anticipated purely from the effect of the bridging hydrogen.⁴¹ In $\text{H}_4\text{Co}_4(\eta^5\text{-C}_5\text{H}_5)_4$, the average Co-Co distance is 2.467 (2) \AA , a value which is close but not strictly comparable to that in our study owing both to the different substituents on the metal atoms and of course the absence of carbonyl bridging groups. Still, the closeness of the values for the average Co-Co distances is noteworthy. In the present structure the face-bridging hydride appears to complete the octahedral geometry about the cobalt atoms; for example, about Co1, H is trans to C1, P1 is trans to Fe, and C4 is trans to C6 (ignoring Co-Co bonds).

Disposition of the $\text{P}(\text{OCH}_3)_3$ Groups. Views along the C_{3v} axis of the molecule are shown in Figure 3; the $\text{P}(\text{OMe})_3$ ligands are spread away from the Co_3 face, presumably to make room for the hydrogen atom. The angle between a P-Co bond and the Co_3 plane is 126° (av). Similar effects are observed in $\text{H}_2\text{Ru}_6(\text{CO})_{18}$;³⁸ the carbonyl groups are spread away from the two faces believed to be bridged by hydrogen while they are observed to be perpendicular to the other triangular faces.

This structure shows many similarities, but a few important differences, when compared to the structures of $\text{Ir}_4(\text{CO})_{12-x}\text{L}_x$ ⁴² ($x = 2, 3$; $\text{L} = \text{PPh}_3$). In all three of these structures the overall geometries are similar (pseudo- C_{3v}) and the bridging carbonyls are less than 10° out of the basal plane. The apical atom in all three compounds has a slightly distorted octahedral environment. In the iridium compounds no significant differences were reported in the metal-metal bond lengths, despite the presence of bridged and unbridged metal-metal bonds. The title compound shows large differ-

Table XII. Shorter Intermolecular Distances^a

First atom	Second atom	Position	Distance, \AA
M21H2 ^b	M33H1	55503	2.502
M22H1	M33H2	56501	2.507
08	M12H1	64503	2.512
02	M21H2	55503	2.581
M21H3	M21H3	55502	2.586
M21H2	M23H2	55502	2.591
M21H3	M23H2	55502	2.601
M11H1	M31H3	65503	2.606
M22H2	M32H3	55502	2.625
023	M21H3	55502	2.634
09	M11H3	65503	2.639
M12H3	M31H3	56501	2.654
05	M33H2	55503	2.661
M12H2	M31H3	56501	2.682
	55503	$-x, 1/2 + y, 1/2 - z$	
	56501	$x, 1 + y, z$	
	64503	$1 - x, y - 1/2, 1/2 - z$	
	55502	$-x, -y, -z$	
	65503	$1 - x, 1/2 + y, 1/2 - z$	

^a Sums of van der Waals radii: H-H, 2.4 \AA ; O-H, 2.6 \AA . ^b MnHm refers to hydrogen in methyl group. Position parameters for group atoms are found in Table VI.

ences between apical-basal and basal-basal distances owing, of course, to the different atoms (Fe and Co) involved and possibly also to the presence of bridging carbonyl ligands in the base. In $\text{Fe}_3(\text{CO})_9(\text{PPh}_3)_3$ ⁴³ the doubly bridged edge is 0.15 \AA shorter than the nonbridged edges.

Perhaps the most interesting difference between the FeCo_3 cluster and the Ir_4 clusters mentioned above concerns the placement of the phosphorus ligands. We may define two types of terminal positions on the basal plane, i.e., axial and equatorial. In $\text{HFeCo}_3(\text{CO})_9\text{L}_3$ all three ligands are axial, while in $\text{Ir}_4(\text{CO})_9\text{L}_3$ only one is axial and two are equatorial. In $\text{Ir}_4(\text{CO})_{10}\text{L}_2$ one ligand is axial and one is equatorial. Perhaps external factors, such as crystal packing, determine the conformation in the solid while the molecules are fluxional in solution.⁴⁴ Of course, the ligand in this study ($\text{P}(\text{OMe})_3$) is much smaller⁴⁵ than the one used with the iridium compounds (PPh_3).

The Tetrahedral Cluster and Its Ligands. In this molecule, as in $\text{Ir}_4(\text{CO})_{12}$ ⁴² and $[\text{H}_6\text{Re}_4(\text{CO})_{12}]^{2-}$,⁴⁶ the three carbonyl groups on Fe are in a staggered conformation with respect to the Co-Co edges (see Figure 3a). This is in contrast to the disposition of the carbonyl groups in $\text{H}_4\text{Re}_4(\text{CO})_{12}$ ³⁷ in which the carbonyl groups are eclipsed with respect to the M-M edges. In this latter compound all four hydride atoms are face-bridging and the disposition of the carbonyl groups is known to be affected by face-bridging ligands.³⁷ In $\text{HFeCo}_3(\text{CO})_9[\text{P}(\text{OCH}_3)_3]_3$ the face-bridging hydride is on the face opposite Fe and thus does not cause the three carbonyl groups on Fe to be eclipsed with respect to the M-M edges.

Bor, Sbrignadello, and Noack have made some predictions about the geometry of $\text{HFeCo}_3(\text{CO})_{12}$ ¹³ based on interaction constants for this compound, $\text{Co}_4(\text{CO})_{12}$, and $\text{Rh}_4(\text{CO})_{12}$. On the basis of the high value of the interaction constant in $\text{HFeCo}_3(\text{CO})_{12}$ between terminal carbonyl carbon on Fe and equatorial terminal carbonyl carbon on Co, the angle C-Fe-C was predicted to be larger than the comparable angle in $\text{Co}_4(\text{CO})_{12}$ and $\text{Rh}_4(\text{CO})_{12}$. In fact, in the title compound C-Fe-C is $96.1 \pm 1.6^\circ$ (av) and is smaller than the C-Co-C angle (101.7°) or the C-Rh-C angle (98.5°). However, in $\text{HFeCo}_3(\text{CO})_9\text{L}_3$ ($\text{L} = \text{P}(\text{OCH}_3)_3$) the equatorial CO groups on Co are bent toward the terminal CO groups on Fe and the positions of all ligands on Co are affected by the face-bridging hydrogen atom. A comparison of the angle Fe-Co-C_{Coeq}

Table XIII. A Comparison of Bond Angles (Averaged) (deg)^a

Atom ^b	HFeCo ₃ (CO) ₉ [P(OCH ₃) ₃] ₃	Co ₄ (CO) ₁₂ ⁴⁰	Rh ₄ (CO) ₁₂ ⁴⁰
Co-Co-Co	60.0 ± .5	60.0 ± 1.7	60.0 ± 1.5
Fe-Co-Co	60.9 ± .1	60.1 ± 0.7	59.6 ± 0.9
Co-Fe-Co	58.1 ± .3	59.8 ± 1.3	60.8 ± 1.3
Co-Fe-C _t Fe	155. ± 1.	151.3 ± 0.6	154.5 ± 2.0
Co-Fe-C _i Fe	101. ± 1.	96.2 ± 2.0	97.9 ± 1.7
Fe-Co-P	174. ± 3.	162.4 ± 5.8	165.0 ± 4.0
Fe-Co-C _e Co	81. ± 3.	92.8 ± 9.8	95.0 ± 6.3
Fe-Co-C _b CO	82. ± 2.	82.6 ± 3.3	79.6 ± 1.9
Co-Co-P	120. ± 5.	105.1 ± 4.3	109.1 ± 5.4
Co-Co-C _b CO	50.4 ± .4	52.6 ± 2.7	46.0 ± 3.4
Co-Co-C _b CO	110. ± 1.	112.6 ± 3.8	106.1 ± 3.6
Co-Co-C _e CO	129. ± 2.	136.8 ± 7.2	137.9 ± 3.5
P-Co-C _b CO	98. ± 2.	95.9 ± 3.1	98.0 ± 8.0
P-Co-C _e CO	98. ± 5.	104.8 ± 8.7	98.5 ± 0.7
C _e CO-Co-C _b CO	95. ± 2.	94.3 ± 5.0	100.4 ± 6.3
C _i Fe-Fe-C _t Fe	96. ± 2.	101.7 ± 2.3	98.5 ± 5.2
Fe-C-O	178.0 ± 0.9	160.6 ± 5.4	167.2 ± 7.6
Co-C _e CO-O	176.8 ± 1.5	163.1 ± 17.6	167.8 ± 10.3
Co-C _b CO-O	140.3 ± .4	140.0 ± 5.9	135.2 ± 7.0
Co-C _b CO-Co	79.1 ± .3	74.6 ± 5.8	87.4 ± 6.3

^a Average values for angles in M₄(CO)₁₂, M = Co, Rh, which correspond to angles in the title compound. The estimated error given is calculated from the formula $[\sum_{i=1}^n (x_i - \bar{x})^2 / (n - 1)]^{1/2}$. ^b tFe refers to a terminal CO on Fe, eCo refers to an equatorial CO on Co, tCo refers to a terminal CO on Co, and bCO refers to a bridging CO.

(81.0°) with the comparable Rh-Rh-C (95.0°) and Co-Co-C (92.8°) reveals this effect. Bor et al.¹³ also find a relatively low stretching force constant for apical CO (terminal CO on Fe) which they attribute to a partial negative charge on Fe and a partial positive charge on H. The location of the hydride atom outside the cluster, away from Fe, is in good agreement with this assumption. An increase in the angle C_{CO}-Co-C_{CO} for the mixed cluster compound is also predicted by Bor et al.¹³ In HFeCo₃(CO)₉L₃ the comparable angle P-Co-C (97.5° av) is not very different from C_{COaxial}-Co-C_{COequatorial} (104.8°) and C-Rh-C (98.5°); in the mixed cluster compound both these ligands on Co shift away from the hydride atom.

The replacement of the axial CO groups on Co in HFeCo₃(CO)₁₂ by P(OCH₃)₃ should not greatly affect the molecular geometry of the cluster and the unsubstituted dodecacarbonyl is probably very similar to the tris-substituted compound. Table XIII includes averaged angles for HFeCo₃(CO)₉[P(OCH₃)₃]₃, Co₄(CO)₁₂, and Rh₄(CO)₁₂. The latter two compounds form disordered crystals, but in almost every case corresponding angles in the three compounds are quite similar. The most noteworthy differences are found in the angles corresponding to Co-Fe-C_{CO(terminalFe)} and C_{CO(terminalFe)}-Fe-C_{CO(terminalFe)} (because the terminal groups on Fe are closer together than those on the apical Co or Rh) and Co-Co-C_{CO(equatorial)}, Co-Co-P, Fe-Co-P, and Fe-Co-C_{CO(equatorial)} (because of the effect of the face-bridging hydride).

Although the effect of bridging hydrides on their associated metal-metal distances is not easy to generalize, in most cases the disposition of ligands around the metal atoms associated with such bridging hydrides is affected. In the title compound, the Co maintains the octahedral configuration and the bridging hydrogen atom occupies one of the six sites.

Acknowledgments. We thank the National Science Foundation for support of this research (Grant CHE76 15436). We also wish to thank Professor W. Dollase of the Department of Geology for use of the Mössbauer spectrometer (NSF Grant DES 74-19918) and Professor C. E. Strouse of this department for help and advice on the use of the Syntex diffractometer with its low-temperature cryostat constructed by him. Computa-

tions were performed at the UCLA Campus Computing Network whom we thank for computer time.

Supplementary Material Available: Tables A-G (mass spectra) and H (structure factor amplitudes for V) and Figures A-F (IR and Mössbauer spectra for I-VI) (31 pages). Ordering information is given on any current masthead page.

References and Notes

- (1) This work was presented in partial fulfillment of the dissertation by B. T. Huie, University of California, Los Angeles, Calif., 1975. (b) A preliminary account has been reported: B. T. Huie, C. B. Knobler, and H. D. Kaesz, *J. Chem. Soc., Chem. Commun.*, 684 (1975).
- (2) P. Chini, L. Colli, and M. Peraldo, *Gazz. Chim. Ital.*, **90**, 1005 (1960).
- (3) C. H. Wei and L. F. Dahl, *J. Am. Chem. Soc.*, **88**, 1821 (1966).
- (4) (a) M. J. Mays and R. N. F. Simpson, *Chem. Commun.*, 1024 (1967); (b) *J. Chem. Soc. A*, 1444 (1968).
- (5) J. Knight and M. J. Mays, *J. Chem. Soc. A*, 711 (1970).
- (6) J. W. White and C. J. Wright, *J. Chem. Soc. A*, 2843 (1971).
- (7) (a) S. A. R. Knox and H. D. Kaesz, *J. Am. Chem. Soc.*, **93**, 4594 (1971); (b) J. W. Koepke, Dissertation, University of California, Los Angeles, 1974.
- (8) C. G. Cooke and M. J. Mays, *J. Chem. Soc., Dalton Trans.*, 455 (1975).
- (9) R. G. Teller, R. D. Wilson, R. K. McMullan, T. F. Koetzle, and R. Bau, *J. Am. Chem. Soc.*, following paper in this issue.
- (10) W. A. Dollase, *Am. Mineral.*, **60**, 257 (1975).
- (11) S. A. R. Knox, J. W. Koepke, M. A. Andrews, and H. D. Kaesz, *J. Am. Chem. Soc.*, **97**, 3942 (1975).
- (12) A. Reckziegel and M. Bigorogne, *J. Organomet. Chem.*, **3**, 341 (1965).
- (13) G. Bor, G. Sbrignadello, and K. Noack, *Helv. Chim. Acta.*, **58**, 815 (1975).
- (14) R. B. King, *Prog. Inorg. Chem.*, **15**, 287-473 (1972).
- (15) Cf. W. Hieber, *Adv. Organomet. Chem.*, **8**, 1-28 (1970), and references cited therein.
- (16) K. Farmery, M. Kilner, R. Greatrex, and N. N. Greenwood, *J. Chem. Soc. A*, 2339 (1969).
- (17) G. M. Bancroft and R. H. Platt, *Adv. Inorg. Chem. Radiochem.*, **15**, 59 (1972).
- (18) "International Tables for X-Ray Crystallography", Vol. I., Kynoch Press, Birmingham, England, 1962.
- (19) C. E. Strouse, *Rev. Sci. Instrum.*, **47**, 871 (1976).
- (20) The programs used in this work included locally written data reduction programs; JBPATT, JBF0UR and PEAKLIST, modified versions of Fourier programs written by J. Blount, local versions of ORFLS (Busing, Martin, and Levy) structure factor calculations and full-matrix least-squares refinement; Hope's HPOSN to calculate tentative hydrogen positions; ORTEP (Johnson), figure plotting; MGTL (Schomaker and Trueblood), analysis of possible rigid-body motion, least-squares planes; ORFFE (Busing, Martin, and Levy), distances, angles, and error computations; CRYM (Reeke), Fourier, general plane; and ABSORB (Coppens), absorption correction. All calculations were performed on the IBM 360-91 computer operated by the UCLA Campus Computing Network.
- (21) C. B. Knobler, S. S. Crawford, and H. D. Kaesz, *Inorg. Chem.*, **14**, 2062 (1975).
- (22) A. J. C. Wilson, *Nature (London)*, **150**, 151 (1942).
- (23) MÜLTAN: P. Main, M. M. Woolfson, and G. Germain, University of York Monograph, Heslington, York, Great Britain, May 1971.

$$(24) \text{ ABS FOM} = \frac{\sum_h \alpha_h - \sum_h \langle \alpha_h^2 \rangle_r^{1/2}}{\langle \alpha_h^2 \rangle_e^{1/2} - \langle \alpha_h^2 \rangle_r^{1/2}}$$

$$\text{RESID} = \frac{\sum_{k_r} | |E_h|_{\text{obsd}} - |E_h|_{\text{calcd}} |}{\sum_{k_r} |E_h|_{\text{obsd}}}$$

- (25) H. P. Hanson, F. Herman, J. D. Lea, and S. Skillman, *Acta Crystallogr.*, **17**, 1040 (1964).
 (26) R. F. Stewart, E. R. Davidson, and W. T. Simpson, *J. Chem. Phys.*, **42**, 3175 (1965).
 (27) The function $\sum w | |F_o| - |F_c| |$ was minimized in the least-squares refinement and the discrepancy indexes were defined as $R_r = (\sum |F_o| - |F_c|) / \sum |F_o|$ and $R_w = [(\sum w (|F_o| - |F_c|)^2) / \sum w |F_o|^2]^{1/2}$, where $w = [1/\sigma(F_o)]^2$.
 (28) D. T. Cromer and D. L. Liberman, *J. Chem. Phys.*, **53**, 1891 (1970).
 (29) C. Scheringer, *Acta Crystallogr.*, **16**, 546 (1963).
 (30) S. J. LaPlaca and J. A. Ibers, *Acta Crystallogr.*, **18**, 511 (1965).
 (31) S. J. LaPlaca and J. A. Ibers, *J. Am. Chem. Soc.*, **85**, 3501 (1963).
 (32) S. W. Kirtley, J. P. Olsen, and R. Bau, *J. Am. Chem. Soc.*, **95**, 4532 (1973).
 (33) (a) W. C. Hamilton, *Acta Crystallogr.*, **18**, 502 (1965); (b) n = number of reflections, m = total number of refineable parameters.
 (34) The estimated error of the mean is calculated using the formula $[\sum \sigma_{x_i}^2]^{1/2}$

- where x_i and \bar{x} are values and mean values, respectively.
 (35) W. C. Hamilton and J. A. Ibers, "Hydrogen Bonding in Solids", W. A. Benjamin, New York, N.Y., 1968, p 64.
 (36) G. Huttner and H. Lorenz, *Chem. Ber.*, **108**, 973 (1975).
 (37) R. D. Wilson and R. Bau, *J. Am. Chem. Soc.*, **98**, 4687 (1976).
 (38) M. R. Churchill, J. Wormald, J. Knight, and M. J. Mays, *Chem. Commun.*, 458 (1970).
 (39) C. R. Eady, B. F. G. Johnson, and J. Lewis, *J. Chem. Soc., Chem. Commun.*, 302 (1976).
 (40) C. H. Wei, *Inorg. Chem.*, **8**, 2384 (1969).
 (41) Minimal effects of hydrogen bridging on bond lengths when accompanied by other atoms also bridging the same elements in a polynuclear structure was first observed in the structure of $\text{HFe}_3(\text{CO})_9\text{SR}$ by R. Bau, B. Don, R. Greatrex, R. J. Haines, R. A. Love, and R. D. Wilson, *Inorg. Chem.*, **14**, 3021 (1975); further examples may be found in the structures of $\text{HO}_3\text{S}(\text{CO})_{10}(\text{CHCH}_2\text{PMe}_2\text{Ph})$, M. R. Churchill and B. G. de Boer, *ibid.*, **16**, 1141 (1977), or $\text{HRu}_3(\text{CO})_{10}(\text{C}=\text{NMe}_2)$, M. R. Churchill, B. G. de Boer, and F. J. Rotella, *ibid.*, **15**, 1843 (1976).
 (42) V. Albano, P. Bellon, and V. Scatturin, *Chem. Commun.*, 730 (1967).
 (43) W. S. McDonald, J. R. Moss, G. Raper, B. L. Shaw, R. Greatrex, and N. N. Greenwood, *Chem. Commun.*, 1295 (1969).
 (44) F. A. Cotton, L. Kruczynski, B. L. Shapiro, and L. F. Johnson, *J. Am. Chem. Soc.*, **94**, 6191 (1972).
 (45) C. A. Tolman, *J. Am. Chem. Soc.*, **92**, 2596 (1970).
 (46) H. D. Kaesz, B. Fontal, R. Bau, S. W. Kirtley, and M. R. Churchill, *J. Am. Chem. Soc.*, **91**, 1021 (1969).
 (47) See paragraph at end of paper regarding supplementary material.

A Neutron Diffraction Study of $\text{HFeCo}_3(\text{CO})_9(\text{P}(\text{OCH}_3)_3)_3$, a Metal Cluster Complex with a Triply Bridging Hydride Ligand

Raymond G. Teller,^{1a,b} Robert D. Wilson,^{1a} Richard K. McMullan,^{1c}
 Thomas F. Koetzle,^{*1c} and Robert Bau^{*1a,d}

Contribution from the Departments of Chemistry, University of Southern California, Los Angeles, California 90007, and Brookhaven National Laboratory, Upton, New York 11973. Received August 20, 1977

Abstract: We wish to report the first accurate neutron diffraction study of a transition metal structure with a triply bridging hydride ligand, the cluster $\text{HFeCo}_3(\text{CO})_9(\text{P}(\text{OCH}_3)_3)_3$. The compound crystallizes in the space group $P2_1/c$, $Z = 4$. The cell constants at 90 K are $a = 15.957$ (8) Å, $b = 10.611$ (5) Å, $c = 18.383$ (9) Å, $\beta = 98.70$ (2)°. The structure was refined, based on the measured intensities of 8229 reflections; the final discrepancy factors for all reflections are $R_{F^2} = 0.087$, $R_{wF^2} = 0.066$. The four metal atoms form a tetrahedron with the apical Fe atom additionally bonded to three terminal carbonyl groups. Each Co atom is further bonded to one terminal and two bridging carbonyl ligands, as well as one phosphite group and the hydride ligand. The hydride ligand is located outside the metal cluster, 0.978 (3) Å from the Co_3 face. This result confirms that of an earlier x-ray investigation by Huie, Knobler, and Kaesz.² The Co-H distances are 1.742 (3), 1.731 (3), and 1.728 (3) Å, and Co-H-Co angles are 92.1 (1), 91.7 (1), and 91.5 (1)°.

Introduction

In 1960, Chini and co-workers reported the isolation of $[\text{FeCo}_3(\text{CO})_{12}]^-$ from the reaction of $\text{Co}_2(\text{CO})_8$ and $\text{Fe}(\text{CO})_5$ in acetone, and the acidification of that anion to form $\text{HFeCo}_3(\text{CO})_{12}$.³ Subsequent investigations by other workers were aimed at elucidating the structure of this interesting cluster, with the location of the H atom being the focus of these experiments. On the basis of mass spectral evidence and electron-counting arguments, Mays and Simpson⁴ in 1968 proposed a structure that placed the H atom inside a tetrahedral "cage" of metal atoms. The arrangement of metal atoms and carbonyl ligands was assumed to be consistent with that of the isoelectronic $\text{Co}_4(\text{CO})_{12}$, the x-ray structure of which was reported by Wei and Dahl⁵ in 1966. This conclusion was later supported by White and Wright,⁶ who, on the basis of inelastic neutron scattering experiments, confirmed the C_{3v} symmetry of the molecule but rejected a structure which contained the hydrogen on or near the Co_3 face of the molecule. The model

proposed by these workers indicated a direct Fe...H interaction. Further interest was stimulated by Bor and co-workers in 1975,⁷ who reaffirmed the C_{3v} symmetry of the molecule but favored a structure which placed the hydrogen near the center of the Co_3 face, in agreement with Chini's original proposal. This conclusion, which was based on IR spectral data, was supported by Mössbauer measurements⁸ which indicated no major structural change about the Fe atom upon deprotonation. A particularly useful aspect of this latest report⁸ was the preparation of some phosphite-substituted derivatives, which form crystals more suitable for diffraction experiments than the parent compound. In 1975, Huie, Knobler, and Kaesz² reported a definitive structure determination of $\text{HFeCo}_3(\text{CO})_9(\text{P}(\text{OCH}_3)_3)_3$ via x-ray crystallography. These workers clearly identified the H atom as being outside the cluster, capping the Co_3 face. However, because of the inherent insensitivity of x-ray data to hydrogen positions, we felt that it would be desirable to have a more accurate measure of the μ_3 -H linkage in this compound. Accordingly, we undertook the